

Combined Single-Crystal X-ray Diffraction and FTIR Study of Morpholinium–Water Molecular Complexes Embedded in a Chabasite Network

Annalisa Martucci,^{*,†} Alberto Alberti,[†] Giuseppe Cruciani,[†] Alberto Frache,[‡] Salvatore Coluccia,[§] and Leonardo Marchese^{*,‡}

Dipartimento di Scienze della Terra, Sezione di Mineralogia, Petrografia e Geofisica, Università di Ferrara, Corso Ercole I d'Este, 32, I- 44100 Ferrara, Italy, Dipartimento di Scienze e Tecnologie Avanzate, Università del Piemonte Orientale "A. Avogadro", C. so Borsalino 54, I-15100 Alessandria, Italy, and Dipartimento di Chimica IFM, Università di Torino, via P. Giuria 7, I-10125 Torino, Italy

Received: February 25, 2003

A combined single-crystal X-ray diffraction (XRD) and FTIR study was performed to define the structures of SAPO-34 and CoAPSO-34 microporous molecular sieves synthesized using morpholine (C_4H_8ONH) as a structure-directing agent and to shed some light on the molecular interactions between molecules embedded within the zeolitic cages after hydrothermal synthesis. All investigated crystals showed a chabasite-related structure that was analyzed in the R-3 space group. The incorporation of Si and Co ions into the aluminophosphate framework was assessed by different procedures (scattering curve refinements and analysis of T–O distances). Silicon-to-phosphorus substitution was within the range of 20–24% Si in the P sites of all SAPO-34 crystals. Conversely, Si-for-P and Co-for-Al substitutions spanned a wider range in CoAPSO-34 crystals. XRD supplemented by TGA analysis showed that 2 morpholine and 2.5–3 water molecules occupied the chabasite cages in all crystals. The presence of morpholinium, $C_4H_8ONH_2^+$ (HM^+), along with morpholine (M) H-bonded to water molecules was detected by FTIR spectroscopy, and a computational study helped to clarify the assignment of the vibrational modes of the isolated organic molecules. The structure of water/morpholinium (or morpholine) molecular complexes, which are formed by $HM^+-H_2O-HM^+$ (or HM^+-H_2O-M) units within the chabasite cages and $HM^+-H_2O-H_2O-HM^+$ (or $HM^+-H_2O-H_2O-M$) chains embedded in the intrazeolite space of adjacent cages of the chabasite network, was refined by single-crystal XRD.

Introduction

Materials with open-framework structures are of great importance in many fields of applied chemistry such as ion exchange, molecular sieving, and catalysis.¹ For this reason, since their discovery in the early 1980s, microporous aluminophosphate ($AlPO_4$) molecular sieves² have been extensively studied in view of their potential use in industrial processes such as catalysis and gas separation.³ These materials and their silico- and metal-substituted analogues^{4–6} have been synthesized in the presence of amines as structure-directing agents that, in some cases, selectively direct crystallization toward a selected framework. Molecular complexes or aggregates of templating molecules may play a decisive role in the formation of the desired materials because they remain embedded inside the inorganic network in the final product. For this reason, a structural study of their location is important.

Many $AlPO_4$ materials are isostructural with zeolites: $AlPO_4$, $AlPO_4$ -44, and $AlPO_4$ -47 in particular have chabasite topology and were prepared in the presence of TEOH (TEOH = tetraethylammonium hydroxide), cyclohexylamine, and *N,N*-diethylethanolamine, respectively.⁷ Other amines such as morpholine have been found to provide chabasite analogues in the

Si–Al–P–O system.^{8–9} When silicon ions are incorporated into the tetrahedral framework sites of AlPOs, selective heterogeneous catalysts are produced.^{8,10} Cosubstituted aluminophosphates are also catalysts that may combine both redox and acidic properties.¹¹ Among these zeotype catalysts, SAPO-34 is highly selective in both methanol-to-olefin (MTO)^{12–14} and oxidative dehydrogenation of ethane (ODH)¹⁵ processes, which are of utmost relevance to the petrochemical industry.

The aim of this single-crystal X-ray diffraction study is threefold: to determine the structures of SAPO-34 and CoAPSO-34, both synthesized in the presence of morpholine, to localize the organic species in the chabasite cages, and to obtain direct evidence of the substitution of Co^{2+} and Si(IV) ions by Al^{3+} and P(V) framework sites, respectively. FTIR spectroscopy was used to monitor the presence of protonated morpholine molecules (e.g., the morpholinium $C_4H_8ONH_2^+$ (HM^+) ion) and their H-bonding interactions with water molecules. Finally, the combined approach of X-ray diffraction and FTIR spectroscopy has permitted a detailed study of the location of morpholinium–water molecular complexes within the chabasite network.

Experimental Section

SAPO-34 was synthesized by mixing 3.26 g of $Al(OH)_3$, 3.46 g of H_3PO_4 (85 wt %), and 10 g of distilled water. The mixture was stirred until a uniform gel was obtained. SiO_2 (0.5 g) and H_2O (10.0 g) were then added, followed by 3.63 g of morpholine

* Corresponding authors. (L.M.) E-mail: leonardo.marchese@unito.it. Tel.: +39-0131-287435. Fax: +39-0131-287416. (A.M.) E-mail: mrs@dns.unife.it. Tel.: +39-0532-293752. Fax: +39-0532-29375.

[†] Università di Ferrara.

[‡] Università del Piemonte Orientale.

[§] Università di Torino.

TABLE 1: Data Collection Parameters

	SAPO-34 (1)	SAPO-34 (2)	SAPO-34 (3)	CoAPSO-34 (1)	CoAPSO-34 (2)
crystal-to-detector distance (mm)	25	25	25	25	25
number of frames for data collection	85	138	57	143	127
exposure time per frame (s)	600	600	1000	600	380
maximum 2θ	55	62	55	55	55
measured reflections	16164	9307	9493	6510	6538
unique reflections	1251	1674	1224	1253	1252
req	0.0289	0.0139	0.0498	0.0358	0.0372

TABLE 2: Refinement Parameters^a

	SAPO-34 (1)	SAPO-34 (2)	SAPO-34 (3)	CoAPSO-34 (1)	CoAPSO-34 (2)
unit cell parameters	$a = 13.809$ (1) Å	$a = 13.794$ (1) Å	$a = 13.774$ (2) Å	$a = 13.809$ (1) Å	$a = 13.800$ (1) Å
	$c = 14.836$ (1) Å	$c = 14.829$ (1) Å	$c = 14.821$ (3) Å	$c = 14.836$ (1) Å	$c = 14.825$ (1) Å
	$V = 2450.03$ Å ³	$V = 2443.56$ Å ³	$V = 2435.16$ Å ³	$V = 2450.03$ Å ³	$V = 2445.03$ Å ³
space group	R-3	R-3	R-3	R-3	R-3
chemical composition			Si _{0.90} Al _{6.00} P _{5.10} O ₂₄ ·2.0M·2.7H ₂ O	Co _{0.80} Al _{5.20} P _{5.42} Si _{0.58} O ₂₄ ·2.0M·2.7H ₂ O	Co _{0.16} Al _{4.84} P _{5.62} Si _{0.38} O ₂₄ ·2.0M·2.7H ₂ O
Z	1	1	1	1	1
reflections with $I > 4\sigma(I)$	1107	1438	990	1049	1004
used in the refinement					
no. of parameters	90	90	90	90	90
largest diffraction peak and hole (e/Å ³)	0.47, -0.45	0.80, -0.69	0.89, -0.85	0.57, -0.43	0.56, -0.54
final R(Fo)	0.046	0.057	0.094	0.051	0.055
final Rw(I)	0.1391	0.1607	0.2469	0.1252	0.1465

^a M = Organic molecule (morpholine or morpholinium)

and 10.0 g of H₂O. CoAPSO-34 was synthesized following a procedure similar to that of SAPO-34 except that 3.00 g of Al(OH)₃ was used instead of 3.26 g and, before adding morpholine, a solution prepared by dissolving 0.664 g of Co(CH₃COO)₂ in 10 g of H₂O was mixed into the gel. The resulting gels (1Al:0.25Si:0.90P:50H₂O:1.25Morph for SAPO-34 and 0.08Co:0.92Al:0.25Si:0.90P:50H₂O:1.25Morph for CoAPSO-34) were crystallized in a static Teflon-lined autoclave under autogenous pressure at 195 °C for 10 days; the crystallinity of as-synthesized samples was verified by XRD powder diffraction using a Philips diffractometer PW1830 and Co K α radiation. The crystal morphology was analyzed by scanning electron microscopy (SEM) on a Leica Stereoscan 420.

Single-crystal X-ray diffraction data were collected at room temperature (Mo K α = 0.71069 Å) on three crystals of SAPO-34 (SAPO-34[1], SAPO-34[2], and SAPO-34[3]) and two crystals of CoAPSO-34 (CoAPSO-34[1] and CoAPSO-34[2]) with different Co/Al ratios using a Nonius Kappa CCD diffractometer equipped with a CCD detector. (See Table 1 for data collection conditions.) The DENZO-SMN¹⁶ package was used for the refinement of unit cell parameters and data reduction. The SHELX-93¹⁷ computer program was used for structure analysis. (See Table 2 for refinement parameters.) Structure refinements of the single crystals were carried out, starting from the crystallographic data reported for the CoAPSO-34 structure,¹⁸ in space group R-3. Atomic scattering factors for neutral atoms were used; curves obtained by interpolating the Si, Al, Co, and P percentages from chemical analysis were employed for T framework sites. H₂O molecules and extraframework ions occupancies were refined using a combination of 3D electron-density synthesis and full matrix least-squares techniques. Anisotropic displacement factors were used for framework atoms (Figure 1), and isotropic displacement factors were used for the other extraframework sites. The position of the morpholine molecules was determined from Fourier and difference Fourier maps. Reasonable values were obtained for C–C, C–O, and C–N bond distances, set free during all stages of refinement. Owing to the strong similarities in all of the

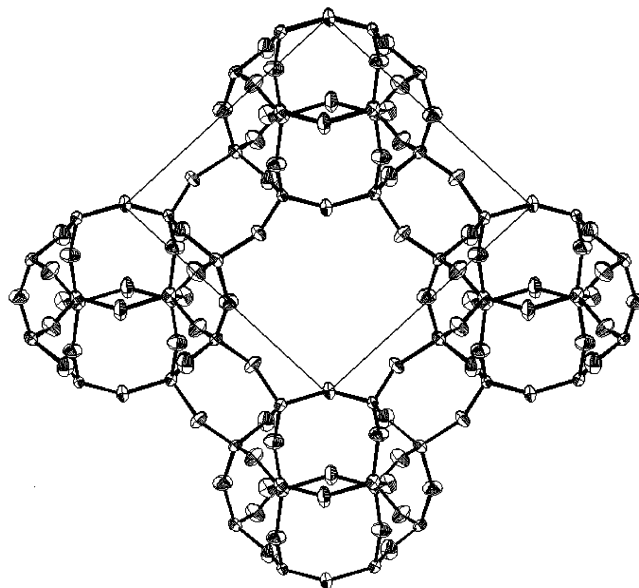


Figure 1. Projection along the [111] direction of the aluminophosphate framework of SAPO-34 showing anisotropically refined atoms.

refined structures, we report only the structural features of SAPO-34[1] and CoAPSO-34[2]. Atomic coordinates, occupancy, and temperature factors are given in Table 3, and bond distances are given in Table 4.

The chemical compositions of SAPO-34[1], CoAPSO-34[1], and CoAPSO-34[2] were determined by an ARL-SEMQ electron microprobe in the wavelength-dispersive mode at 15 KV with a 20-nA sample current and defocused beam (20 μ m) on the same crystals used for the X-ray data collection. For each sample, three to five point analyses were performed. The chemical formulas are reported in Table 2.

TGA analyses of SAPO-34 and CoAPSO-34 were carried out on a TA instrument (SDT2960 model) by keeping 10–15 mg of as-synthesized samples under a constant air flux and using a temperature rate of 20 °C/min. FTIR spectra (resolution 4

TABLE 3: Atomic Coordinates and Fractions for SAPO-34 and CoAPSO-34, Respectively

	SAPO-34					CoAPSO-34				
	<i>x/a</i>	<i>y/b</i>	<i>z/c</i>	U_{eq}^a U_{iso}^*	or Occ.	<i>x/a</i>	<i>y/b</i>	<i>z/c</i>	U_{eq}^a U_{iso}^*	or Occ.
T1	−0.0031(1)	0.2256(1)	0.1034(1)	0.0210(3)	1	−0.0041(1)	0.2250(1)	0.1024(1)	0.0321(4)	1
T2	0.2245(1)	0.2280(1)	0.1088(1)	0.0178(3)	1	0.2230(1)	0.2280(1)	0.1110(1)	0.0319(4)	1
O1	−0.0040(2)	0.2551(2)	−0.0091(2)	0.0369(6)	1	−0.0053(2)	0.2536(3)	0.0129(2)	0.0582(9)	1
O2	0.1227(2)	0.2389(2)	0.1354(2)	0.0341(6)	1	0.1230(3)	0.2392(3)	0.1370(2)	0.0581(9)	1
O3	0.1956(2)	0.1064(2)	0.1271(2)	0.0374(6)	1	0.1940(3)	0.1078(2)	0.1283(2)	0.0581(9)	1
O4	0.3429(2)	0.0236(2)	0.1655(2)	0.0320(6)	1	0.3466(2)	0.0260(3)	0.1630(2)	0.0591(9)	1
Om1	0	0	0.282(1)	0.106(5)	0.3333	0	0	0.288(1)	0.193(6)	0.3333
N	−0.053(3)	−0.130(3)	0.432(3)	0.17(1)	0.3333	−0.045(2)	−0.131(2)	0.435(2)	0.16(1)	0.3333
C1	0.055(3)	−0.023(3)	0.323(2)	0.121(9)	0.3333	0.082(3)	−0.016(3)	0.337(3)	0.14(1)	0.3333
C2	0.121(3)	0.004(4)	0.365(3)	0.15(1)	0.3333	0.129(3)	0.004(4)	0.395(3)	0.14(1)	0.3333
C3	−0.012(4)	−0.111(3)	0.353(3)	0.15(1)	0.3333	0.002(3)	−0.103(3)	0.348(3)	0.18(2)	0.3333
W1	0.098(2)	−0.114(2)	0.369(1)	0.17(1)	0.35(2)	0.100(2)	−0.120(2)	0.372(2)	0.17(1)	0.35(2)
W2	0	0	0.066(6)	0.16(3)	0.14(1)	0	0	0.02(2)	0.19(8)	0.09(8)
W3	0.1667	−0.1667	0.3333	0.18(4)	0.08(1)	0.1667	−0.1667	0.3333	0.17(4)	0.06(1)

$$^a U_{\text{eq}} = (U_{11} + U_{22} \sin^2 \beta + U_{33} + 2U_{13} \cos \beta) / [3(1 - \cos^2 \beta)].$$

TABLE 4: Selected Bond Distances (Å) and Angles (deg) for SAPO-34 and CoAPSO-34, Respectively

SAPO-34				CoAPSO-34			
T1–O1	1.720(2)	T2–O1	1.540(2)	T1–O1	1.756(3)	T2–O1	1.518(3)
T1–O2	1.719(2)	T2–O2	1.538(2)	T1–O2	1.743(3)	T2–O2	1.516(3)
T1–O3	1.738(3)	T2–O3	1.543(2)	T1–O3	1.768(3)	T2–O3	1.522(3)
T1–O4	1.722(2)	T2–O4	1.540(2)	T1–O4	1.744(3)	T2–O4	1.518(3)
T1–O1–T2	150.0(2)	Om1–C1 [×2]	1.13(3)	T1–O1–T2	150.4(3)	Om1–C1 [×2]	1.47(4)
T1–O2–T2	147.5(2)	C1–C2	1.03(4)	T1–O2–T2	146.2(2)	C1–C2	1.01(5)
T1–O3–T2	145.8(2)	N–C2	1.48(5)	T1–O3–T2	144.8(2)	N–C2	1.27(4)
T1–O4–T2	146.2(2)	N–C3	1.28(5)	T1–O4–T2	146.4(2)	N–C3	1.39(5)
		C1–C3	1.19(4)			C1–C3	1.17(4)

cm^{-1}) of pelleted samples were recorded in transmittance mode on an ATI Mattson research series spectrometer equipped with a high-vacuum, variable-temperature infrared cell (LB-100 by Infraspac Ltd, Novosibirsk, Russia). The spectra obtained after heating the samples from 300 to 823 K are presented on the absorbance scale. The main vibrational modes of isolated morpholine molecules and the morpholinium ion were computed using the Gaussian 98¹⁹ program at the BLYP level using the 6-31G(d,p) basis set and were represented by the MOLDRW program.²⁰

Results and Discussion

Materials Characterization. Scanning electron microscopy showed that all crystals have pseudocubic rhombohedral morphology. The average crystal size was in the range of 20–50 μm , although in some cases very large, regularly shaped crystals suitable for X-ray single-crystal analysis were also observed.

Thermogravimetric analysis (TGA) was used to determine the number of molecules embedded inside the chabasite cages of SAPO-34 and to monitor the decomposition processes of organic molecules during the heating procedure required to eliminate the templating agent and activate the catalyst.^{8,15} We used a similar approach to study CoAPSO-34 samples, prepared by adapting the preparation route proposed for SAPO-34.⁸ The first weight loss (around 5%), which occurred at 300–473 K, was due to water molecules eliminated from the cages, whereas the second weight loss (around 17%), in the range of 473–973 K, was due to the decomposition and elimination of the organic template (morpholine). From these data, it may be computed that 2 morpholine molecules and 2.5–3 water molecules are located within the chabasite cages. From chemical analyses reported in Table 2, the charge imbalance in the framework was around 1.3–1.4. Therefore, about $2/3$ of the organic molecule must be protonated (e.g., the morpholinium $\text{C}_4\text{H}_8\text{ONH}_2^+$ (HM^+))

ion), whereas the residual $1/3$ was morpholine, $\text{C}_4\text{H}_8\text{ONH}$. Indeed, clear-cut evidence for the presence of morpholinium was found by FTIR spectroscopy (see below). However, because the organic content was higher than that necessary to balance the net framework charge, we must suppose that part of the molecules are unprotonated.

Structure Refinement. SAPO-34 and isostructural SAPO-47 have been studied by Ito et al.²¹ and Pluth and Smith,²² respectively; the former was synthesized in the presence of morpholine, and the latter, in the presence of methylbutylamine as a structure-directing agent. Only the coordinates of the framework atoms are reported by Ito et al.,²¹ who refined the crystal structure in the acentric R-3 space group. The centric R-3 space group was assumed by Pluth and Smith,²² who found that the encapsulated organic species were strongly disordered. The crystal structure of CoAPSO-34, synthesized with *i*-propylamine as a structure-directing agent, was refined by Nardin et al.¹⁸, whereas CoAPO-44, CoAPO-47, CoAPSO-44, and CoAPSO-47 in the presence of cyclohexylamine molecules were refined by Bennet and Marcus²³ using X-ray single-crystal diffraction in the P-1 space group. The amine molecules were located inside the chabasite cages. In all of these structures, Si and Co isomorphously substituted P and Al respectively in the tetrahedral sites.

In our crystals, the incorporation of Si and Co in tetrahedral sites was assessed by the following:

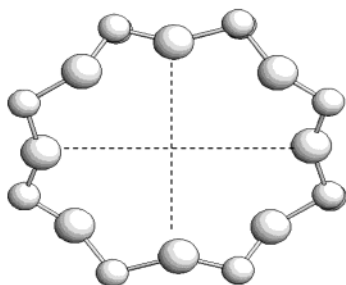
(a) An analysis of the T–O bond distances. For Si–O, we assumed the value of 1.603 Å found in the purely siliceous chabasite;²⁴ for Al–O, the value of 1.725 Å found in the structurally related SAPO-47 structure;²² and for Co–O and P–O, the values 1.93 and 1.52 Å, respectively.²⁵

(b) The Co and Al occupancies in the T1 site, obtained by scattering curve refinements.

In SAPO-34 crystals, the average T–O distances for the T1 and T2 tetrahedra were 1.725 and 1.538 Å, respectively.

TABLE 5: Comparison of Pore-Size Values for Chabasite-like Materials

free diameter (Å) of the eight-membered ring viewed normal to [001]

SAPO-34 (this work), synthesized with morpholine: 4.01×3.60 Å.SAPO-34,²¹ synthesized with morpholine: 4.02×3.61 Å.CoAPSO-34,¹⁸ synthesized with *i*-propylamine: 3.85×3.64 Å.SAPO-47,²² synthesized with methylbutylamine: 3.78×3.82 Å.

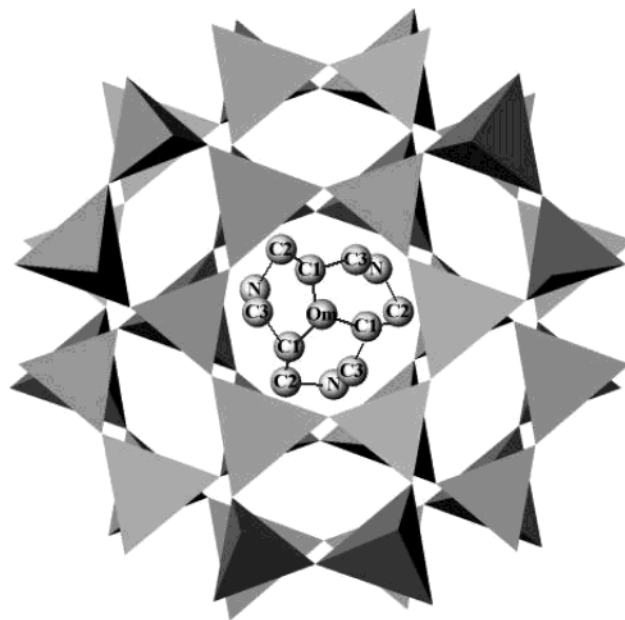
According to criterion a, the T2 site was occupied by 78% P and 22% Si, in excellent agreement with the results of Pluth and Smith.²² The two crystals of CoAPSO-34 differed mainly in their Co and Si contents in the tetrahedral sites. One of these, in accordance with criteria a and b, showed about 15% Co in T1 but no Si in T2, whereas the other crystal was characterized by about 10% Co in T1 and 5% Si in T2. According to the chemical analyses, the Al tetrahedron was occupied by 19% Co, and the P tetrahedron was occupied by 5% Si in the first crystal, whereas in the second one the two tetrahedra were occupied by 15% Co and 9% Si, respectively.

The presence of encapsulated organic species caused a remarkable distortion of the eight-membered rings. (See Table 5 for details.) As can be clearly seen in Table 5, the ring shape became strongly elliptical in the presence of morpholine (this work and Ito et al.²¹) when compared with that found in the presence of methylbutylamine²² or *i*-propylamine.¹⁸

Two organic molecules (morpholine or morpholinium) were localized, by electron density maps, inside the chabasite cages in all structure refinements of both SAPO-34 and CoAPSO-34 crystals. Each of these occupied three different positions, with $1/3$ occupancy rotated around the 3-fold axis and the oxygen atom placed (Om in Table 3) as a pivot on the triad (Figure 2). Obviously, only one of these three positions can be occupied at a time. Morpholine or morpholinium ions assumed a chair shape. Our Om site corresponds to the half-occupied water molecule site found by Nardin et al.,¹⁸ whereas these authors located the organic molecule roughly at the center of the eight-membered ring. The location of *i*-propylamine is very similar to that of the disordered cyclohexylamine found in CoAPO-44²³ and is not far from the methylbutylamine in SAPO-47.²² As discussed below, water molecule W1 in our crystals is placed near the center of the eight-membered rings. This result explains the different shape of the eight-membered rings shown in Table 5, which is related to the presence of morpholine in comparison with other amines.

The two organic molecules are related by the inversion center in the middle of the cage. The large distance between them prevented their interaction via H-bonding. The high-temperature factors of all atoms of the organic molecules could be interpreted as being due either to a real dynamic disorder or to a static disorder around the center of gravity. Because the temperature factors are very similar in all of the refined structures, it seems highly probable that they are due to dynamic disorder.

Three additional extraframework sites have been localized and are attributed to water molecules. Two of these (W2 and

**Figure 2.** Projection along the [111] direction of the chabasite cage showing the organic molecules in SAPO-34 and CoAPSO-34.

W3) are weakly occupied, and the third (W1) has $1/3$ occupancy, which is the same as that for organic molecules, in all of the crystals studied. The importance of this feature is immediately clear: the distances of all atoms of the organic molecules from the framework oxygens are always greater than 3.3 Å, indicating that they are only weakly bonded, if at all, to the framework. On the contrary, the distances of the organic molecule from W1 (3.11 and 2.84 Å, respectively) suggest that different morpholine or morpholinium ions could be connected by means of hydrogen bonds through W1 to form a chain of morpholinium (or morpholine) ions and water molecules. The same occupancy of W1 and organic molecules supports this assumption. In particular, the two organic molecules related by the inversion center within the chabasite cage are connected to each other through W1 water molecules, as shown in Figure 3a, to form $\text{HM}^+ - \text{H}_2\text{O} - \text{HM}^+$ (or $\text{HM}^+ - \text{H}_2\text{O} - \text{M}$) molecular complexes. At the same time, morpholinium–water (or morpholine–water) molecular complexes of adjacent chabasite cages can be connected by hydrogen bonds to symmetrically equivalent water molecules in W1 sites to form $\text{HM}^+ - \text{H}_2\text{O} - \text{H}_2\text{O} - \text{HM}^+$ (or $\text{HM}^+ - \text{H}_2\text{O} - \text{H}_2\text{O} - \text{M}$) chains (Figure 3b). On the basis of the structural data described here, the existence of interactions between water–water molecules ($\text{H}_2\text{O} - \text{H}_2\text{O}$) and morpho-

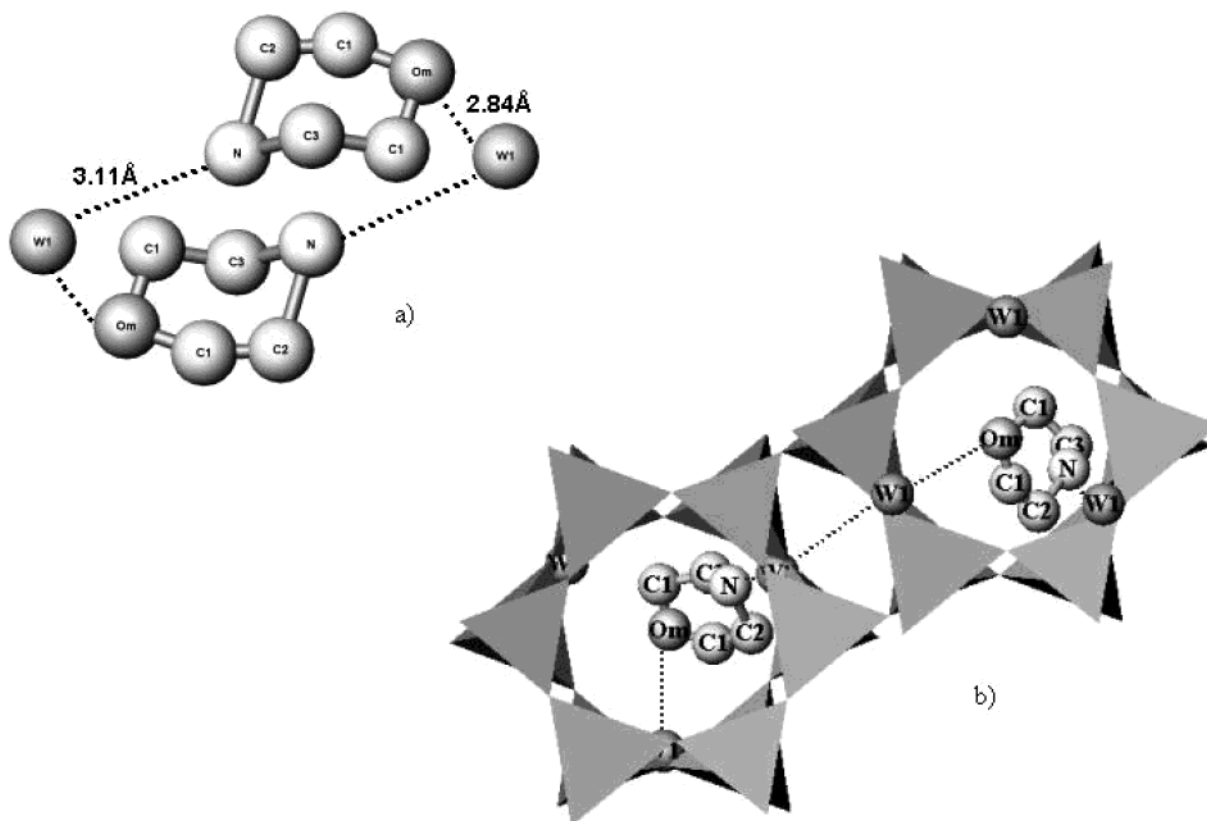
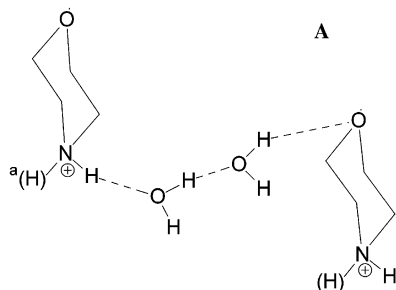


Figure 3. (a) Morpholinium–water (or morpholine–water) molecular complexes localized in a chabasite cage. (b) Molecular complexes of adjacent chabasite cages connecting each other by hydrogen bonds to symmetrically equivalent water molecules at the W1 sites to form HM⁺–H₂O–H₂O–HM⁺ (or HM⁺–H₂O–H₂O–M) chains.

SCHEME 1 ^a



^a Parentheses indicate the possibility that the molecule is protonated or neutral.

linium–water (or morpholine–water) molecules of the type represented in Scheme 1 is proposed; this result is definitively confirmed by the FTIR spectroscopic study reported below.

Molecular Interactions in the Chabasite Network: An FTIR Study. FTIR spectroscopy was used to monitor which types of interaction occur between water and/or morpholine molecules (host–host interactions) trapped within the chabasite cages as well as other interactions, if any, between these molecules and the zeolitic framework (host–guest interactions).⁸ Figure 4A shows FTIR spectra of as-synthesized CoAPSO-34 recorded after outgassing at temperatures of 300 to 473 K (curves 1–4). The spectrum of the sample obtained after removing the organic species at 823 K in oxygen (curve 5) is also reported for comparison because it shows only the typical bands of bridging OH groups at 3624 and 3602 cm^{−1} for acid SAPO-34 catalysts^{26,27} that are overlapped with the scattering profile of the microcrystalline solid.²⁸

It should first be noted that the low-wavenumber region (1750–1250 cm^{−1}) is dominated by the vibrational features of morpholinium, C₄H₈ONH₂⁺, as revealed by the typical NH₂ scissoring mode (Scheme 2 and Table 6) absorbing at 1610 cm^{−1} (Figure 4B, curve 4).²⁹ Absorptions with low intensity might be related to neutral morpholine, which represents only a minor fraction of the organic molecules within the chabasite cages. Computational calculations, performed by Gaussian 98, were used to assign the main absorptions of morpholinium, and these will be discussed in the following text with particular emphasis on the vibrational modes affected by molecular interactions with water.

The spectrum at 300 K shows two intense, broad bands in the 3800–3400 and 3400–1750 cm^{−1} regions, which undoubtedly revealed the presence of a large extension of OH...O- and NH...O-type H-bond interactions. The absorption in the 3800–3400 cm^{−1} range, which decreased upon increasing evacuation temperature and completely disappeared after treatment at 473 K, can be easily assigned to O–H...O vibrations of H-bonded water molecules. The H₂O bending mode is found at around 1620 cm^{−1}, heavily overlapping the NH₂ scissoring mode of morpholinium, and disappears in conjunction with the 3800–3400 cm^{−1} absorption.

Broad bands in the 3300–1750 cm^{−1} region can be safely assigned to stretching vibrations of NH₂ groups of the morpholinium H-bonded to water molecules, according to the XRD data. (The NH group of the morpholine H-bonded to water also absorbs in this region.) Scheme 1 (structure A) shows an arrangement of morpholinium and water molecules that is in agreement with both the single-crystal XRD data and spectroscopic results. However, absorptions at 3300–1750 cm^{−1} are still present after outgassing at 473 K, and this is a strong

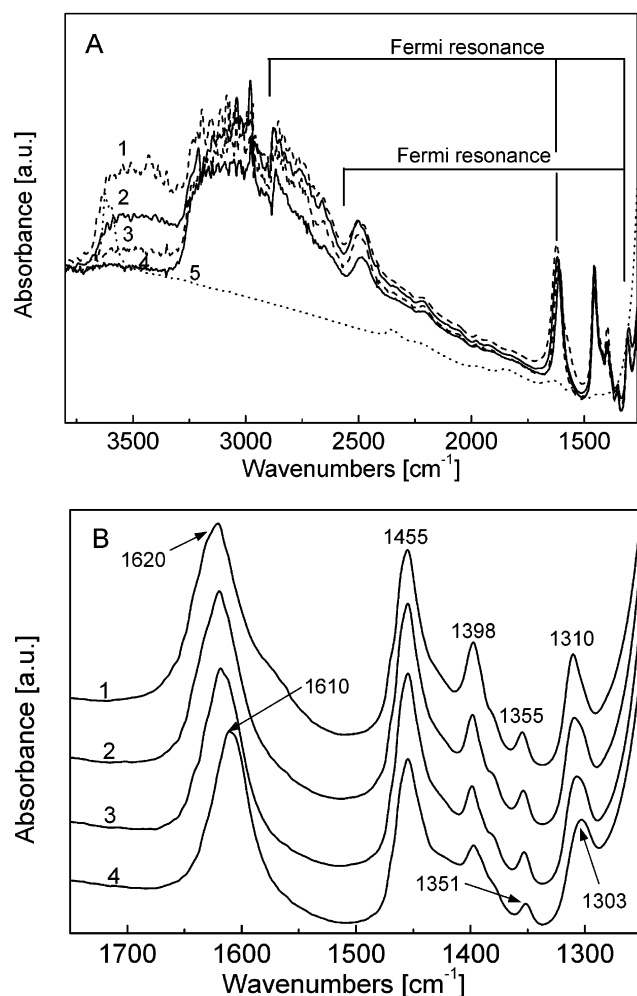
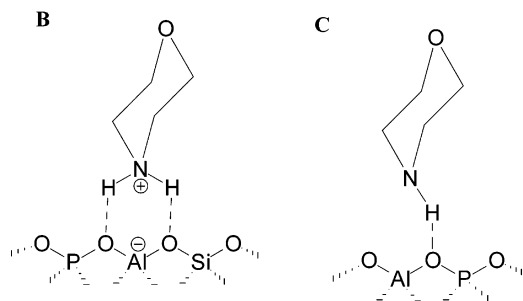


Figure 4. (A) FTIR spectra of as-synthesized CoAPSO-34 recorded after outgassing at 298, 323, 373, and 473 K (curves 1–4, respectively). The spectrum of the sample obtained after removing the organic species at 823 K in oxygen is also reported (curve 5, dotted line). (B) Expanded view of the 1750–1250 cm^{-1} region.

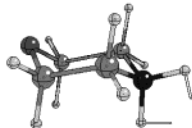
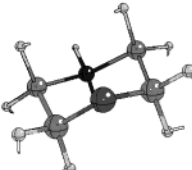
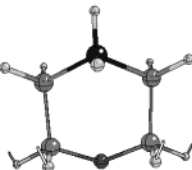
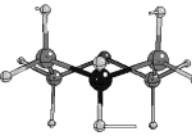

SCHEME 2



indication that, after water removal, morpholinium ions (or morpholine molecules) H-bond to framework oxygens via NH_2 (or NH for the morpholine) groups (Scheme 2, structures B and C).

The evolution of the NH_2 bending modes of morpholinium upon outgassing at increasing temperature confirmed this hypothesis. The IR spectrum of the CoAPSO-34 sample outgassed at 300 K showed a complex band at around 1620 cm^{-1} (Figure 4B, curve 1) where the deformation mode of water absorbed, heavily overlapping the NH_2 scissoring vibration of the morpholinium ion. Upon increasing the outgassing temperature, the band decreased in intensity as water molecules were eliminated from the chabasite cages, and the maximum of the

TABLE 6: Schematic Representation of the Normal Modes of Morpholinium, Computed by Gaussian 98, with Their Vibrational Wavenumbers

observed wavenumber (cm^{-1})	normal modes	
1610		NH_2 scissoring
1455		CH_2 scissoring
1398		CH_2 in-plane deformation
1351		NH axial deformation
1303		NH equatorial deformation

band gradually shifted to lower wavenumbers. Similar shifts occurred for two bands at 1355 and 1310 cm^{-1} , assigned to complex deformation modes of the morpholinium ring where NH axial and NH equatorial bonds are mainly involved. In the absence of water, these bands were found at 1351 and 1303 cm^{-1} (Table 6). These results can be explained by considering that when NH_2 groups are H-bonded to water their wavenumbers shift to higher values, thus revealing that oxygen atoms of water molecules have a different basicity than oxygens of the framework.

CH_2 deformation modes at 1455 and 1398 cm^{-1} were not affected upon increasing the evacuation temperature because these groups do not give significant H-bond interactions. The main deformation modes of the isolated morpholinium ion are represented in Table 6.

The presence of two bands at 2866 and 2500 cm^{-1} overlapping the broad absorption of the H-bonded NH_2 groups in the 3300–1750 cm^{-1} range, together with their evolution as a function of temperature variation, can now be better understood. The shape of the 3300–1750 cm^{-1} absorption is similar to that obtained by NH_3 adsorption on H-SAPO-34, where Evans windows produced by Fermi resonance interactions were detected.^{30,31} In the present case, the overtone of the NH equatorial bending mode ($2\nu_{\text{NHeq}} = 2620 \text{ cm}^{-1}$) as well as the combination of NH_2 scissoring and NH equatorial modes ($\nu_{\text{NH}_2\text{sciss.}} + \nu_{\text{NHeq}} = 2920 \text{ cm}^{-1}$) may lead to Fermi resonance

interactions with the fundamental stretching vibrations of the H-bonded NH_2 groups, thus producing two Evans windows at around 2550 and 2900 cm^{-1} .

The bands at 2866 and 2500 cm^{-1} are therefore false maxima generated by Fermi resonance effects. This assignment is also supported by the fact that, upon water removal, these maxima (together with the Evans windows) shift to lower wavenumbers similarly to the fundamental NH_2 bending vibrations; this effect is more clearly visible in the case of the maximum at 2500 cm^{-1} . Stretching vibrations of CH_2 groups may also contribute to the band at around 2900 cm^{-1} ; however, the presence of resonance effects does not allow the real position of this absorption to be defined.

Conclusions

Si and Co were substituted for P and Al ions, respectively, in tetrahedral sites of SAPO-34 and CoAPSO-34 materials with a chabasite-related structure, which also showed a remarkable flexibility of the framework as a function of the encapsulated structure-directing agent. Two organic molecules (morpholinium and morpholine) were localized inside the chabasite cages; these may occupy three different positions rotated by 120° around the 3-fold axis, with the oxygen atom placed as a pivot on the triad. Framework oxygens are far from the organic molecules (distances greater than 3.3 Å), and this prevents strong interactions between the inorganic network and morpholinium (and/or morpholine). The presence of water molecules close to the center of the eight-membered rings (W1 sites) and their proximity to the morpholinium ions (distance 2.84 and 3.11 Å) suggest that $\text{HM}^+-\text{H}_2\text{O}-\text{HM}^+$ (or $\text{HM}^+-\text{H}_2\text{O}-\text{M}$) complexes are located inside each chabasite cage. H-bonds between $\text{H}_2\text{O}-(\text{W1})-\text{H}_2\text{O}(\text{W1})$ molecules connect these complexes to form $\text{HM}^+-\text{H}_2\text{O}-\text{H}_2\text{O}-\text{HM}^+$ (or $\text{HM}^+-\text{H}_2\text{O}-\text{H}_2\text{O}-\text{M}$) chains embedded within the chabasite network; these may extend throughout several cages.

FTIR spectroscopy monitored the presence of morpholinium ions within the chabasite cages and the occurrence of water–water and water–morpholinium interactions. This result, in combination with the structural data refined by single-crystal X-ray analysis, indicated the occurrence of unique molecular complexes within the zeolitic network of SAPO-34 and CoAPSO-34. It is proposed that $\text{HM}^+-\text{H}_2\text{O}-\text{HM}^+$ (or $\text{HM}^+-\text{H}_2\text{O}-\text{M}$) molecular complexes are the structure-directing agents of the chabasite cages and that the $\text{HM}^+-\text{H}_2\text{O}-\text{H}_2\text{O}-\text{HM}^+$ (or $\text{HM}^+-\text{H}_2\text{O}-\text{H}_2\text{O}-\text{M}$) chains extending along the zeolitic structure are the building units of the supramolecular architecture of the chabasite framework.

Acknowledgment. Italian CNR and MURST (Catalysis for the Reduction of the Environmental Impact of Mobile Source Emissions, COFIN2000, and Zeolites, Materials of Interest for Industry and Environment: Synthesis, Crystal Structure, Stability and Applications, COFIN 2001) are acknowledged for financial support. We thank Dr. G. Croce for assistance in the use of the Gaussian 98 program.

References and Notes

- (1) Corma, A. *Chem. Rev.* **1997**, 97, 2373–2419.
- (2) Wilson, S. T.; Lok, B. M.; Messina, C. A.; Cannan, T. R.; Flanigen, E. M. *J. Chem. Soc.* **1982**, 104, 1146–1147.
- (3) Thomas, J. M. *Angew. Chem., Int. Ed.* **1999**, 38, 3588–3628.
- (4) Wilson, S. T.; Flanigen, E. M. U.S. Patent 4,567,029, 1986.
- (5) Messina, C. A.; Lok, B. M.; Flanigen, E. M. U.S. Patent 4,544,143, 1982.
- (6) Wright, L. J.; Milestone, N. B. *Eur. Pat. Appl.* 0141662, 1985.
- (7) Feng, P. F.; Bu, X.; Gier, T. E.; Stucky, G. D. *Microporous Mesoporous Mater.* **1998**, 23, 221–229.
- (8) Marchese, L.; Frache, A.; Gianotti, E.; Martra, G.; Causà, M.; Coluccia, S. *Microporous Mesoporous Mater.* **1999**, 30, 145–154.
- (9) Prakash, A. M.; Unnikrishnan, S. *J. Chem. Soc., Faraday Trans.* **1994**, 90, 2291–2296.
- (10) Xu, Y.; Grey, C. P.; Thomas, J. M.; Cheetham, A. K. *Catal. Lett.* **1990**, 4, 251–260.
- (11) Frache, A.; Palella, B.; Cadoni, M.; Pirone, R.; Ciambelli, P.; Pastore, H. O.; Marchese, L. *Catal. Today* **2002**, 75, 359–365.
- (12) Thomas, J. M. *Angew. Chem., Int. Ed. Engl.* **1994**, 33, 910–913.
- (13) Stöcker, M. *Microporous Mesoporous Mater.* **1999**, 29, 3–48.
- (14) Chen, J. S.; Thomas, J. M. *Chem. Commun.* **1994**, 603–604.
- (15) Marchese, L.; Frache, A.; Gatti, G.; Coluccia, S.; Lisi, L.; Ruoppolo, G.; Russo, G.; Pastore, H. O. *J. Catal.* **2002**, 208, 479–484.
- (16) Haddad, M. S.; Schimandle, J. J. *Eur. Patent* 234755, 1987.
- (17) Sheldrick, G. M. *SHELXL-93*; University of Göttingen: Göttingen, Germany, 1993.
- (18) Nardin, G.; Randaccio, L.; Kaucic, V.; Rajic, N. *Zeolites* **1991**, 11, 192–194.
- (19) Frisch, M. J.; Trucks, G. W.; Schlegel, H. B.; Scuseria, G. E.; Robb, M. A.; Cheeseman, J. R.; Zakrzewski, V. G.; Montgomery, J. A., Jr.; Stratmann, R. E.; Burant, J. C.; Dapprich, S.; Millam, J. M.; Daniels, A. D.; Kudin, K. N.; Strain, M. C.; Farkas, O.; Tomasi, J.; Barone, V.; Cossi, M.; Cammi, R.; Mennucci, B.; Pomelli, C.; Adamo, C.; Clifford, S.; Ochterski, J.; Petersson, G. A.; Ayala, P. Y.; Cui, Q.; Morokuma, K.; Malick, D. K.; Rabuck, A. D.; Raghavachari, K.; Foresman, J. B.; Cioslowski, J.; Ortiz, J. V.; Stefanov, B. B.; Liu, G.; Liashenko, A.; Piskorz, P.; Komaromi, I.; Gomperts, R.; Martin, R. L.; Fox, D. J.; Keith, T.; Al-Laham, M. A.; Peng, C. Y.; Nanayakkara, A.; Gonzalez, C.; Challacombe, M.; Gill, P. M. W.; Johnson, B. G.; Chen, W.; Wong, M. W.; Andres, J. L.; Head-Gordon, M.; Replogle, E. S.; Pople, J. A. *Gaussian 98*; Gaussian, Inc.: Pittsburgh, PA, 1998.
- (20) Ugliengo, P.; Viterbo, D.; Chiari, G. Z. *Kristallogr.* **1993**, 207, 9–23. Available at <http://www.chimifm.unito.it/fisica/moldraw/moldraw.html>.
- (21) Ito, M.; Shimoyama, Y.; Saito, Y.; Tsurita, Y.; Otake, M. *Acta Crystallogr., Sect. C* **1985**, 41, 1698–1700.
- (22) Pluth, J. J.; Smith, J. V. *J. Phys. Chem.* **1989**, 93, 6516–6520.
- (23) Bennet, J. M.; Marcus, K. *Stud. Surf. Sci. Catal.* **1988**, 37, 269–279.
- (24) Díaz-Cabanas, M. J.; Barrett, P. A.; Cambor, M. A. *Chem. Commun.* **1998**, 1881–1882.
- (25) Shannon, R. D. *Acta Crystallogr., Sect. A* **1976**, 32, 751–753.
- (26) Smith, L.; Cheetham, A. K.; Marchese, L.; Gianotti, E.; Thomas, J. M.; Wright, P. A.; Chen, J. *Catal. Lett.* **1996**, 41, 13–16.
- (27) Smith, L.; Marchese, L.; Cheetham, A. K.; Thomas, J. M.; Wright, P. A.; Chen, J.; Morris, R. E. *Science* **1996**, 271, 799–802.
- (28) Marchese, L.; Martra, G.; Coluccia, S. *Microcrystalline Materials Characterized by Infrared Spectroscopy*. In *New Trends in Materials Chemistry*; Catlow, R.; Cheetham, A., Eds.; NATO ASI Series; Kluwer Academic Publishers: Norwell, MA, 1997; Vol. 498, pp 79–109.
- (29) Lin-Vien, D.; Colthup, N. B.; Fateley, W. G.; Grasselli, J. G. *The Handbook of Infrared and Raman Characteristic Frequencies of Organic Molecules*; Academic Press: Boston, MA, 1991.
- (30) Zecchina, A.; Marchese, L.; Bordiga, S.; Pazè, C.; Gianotti, E. *J. Phys. Chem. B* **1997**, 101, 10128–10135.
- (31) Coluccia, S.; Marchese, L.; Martra, G. *Microporous Mesoporous Mater.* **1999**, 30, 43–56.